Reliability Engineering and System Safety 215 (2021) 107735

Contents lists available at ScienceDirect

Reliability Engineering and System Safety

journal homepage: www.elsevier.com/locate/ress

A hierarchical Bayesian approach for assessing infrastructure networks serviceability under uncertainty: A case study of water distribution systems

Jin-Zhu Yu [a], Mackenzie Whitman [a], Amirhassan Kermanshah [b], Hiba Baroud [a,*]

[a] Vanderbilt University, United States of America
[b] Sharif University of Technology, Iran

ARTICLE INFO

Keywords:
Uncertainty quantification
Data scarcity
Infrastructure Systems
Importance ranking
Network performance
Component functionality

ABSTRACT

Measuring the performance of infrastructure networks is critical to the allocation of resources before, during, and after a system's disruption. However, the lack of data often hinders the ability to accurately estimate infrastructure performance, resulting in uncertainty in its evaluation which can lead to biased estimates. To address this challenge, this study develops a Bayesian approach to measure the performance of the infrastructure network at the component level and incorporate it in the evaluation of the system-level serviceability. Component fragility metrics are estimated using a hierarchical Bayesian model and then integrated into the system serviceability assessment using Monte Carlo simulation and a shortest-path algorithm. These performance measures can be dynamically updated as more data becomes available. A case study of the water distribution system of Shelby County in Tennessee subject to earthquake and flood hazards is presented to illustrate the proposed approach. Results show that system topology is more important in determining component functionality under seismic hazard while vulnerability is the dominant factor in the case of flood hazard.

1. Introduction

Critical infrastructure systems (CISs) such as power grids, water distribution systems, telecommunication networks, and transportation systems provide essential services to modern society [1]. These systems have grown in scale and complexity due to urbanization and technology advancement. Additionally, they are increasingly threatened by a wide range of natural (e.g., extreme weather events) and anthropogenic (e.g., man-made attacks) hazards. The U.S. government has emphasized the protection of CISs by improving their ability to withstand and recover from all hazards as they are considered paramount to national security [2]. The protection of CISs relies on risk-informed decision making to identify strategies for hardening, emergency response, and restoration. To inform such decisions, it is essential to provide a reliable assessment of the system-level performance of CISs under different types of hazards. This study presents an approach to assess the serviceability of CISs during disasters with a focus on water distribution systems (WDSs) impacted by earthquakes and floods. Water distribution systems are credited to be one of the most essential types of infrastructure, especially during a disaster when reduced water supply disrupts the emergency response (e.g., first-aid) and residential and industrial activities, among others [3]. However, among the CISs that are vulnerable to earthquake and flood [4], WDSs have been overlooked and undervalued in the U.S. in the past decade [5]. In addition, research advances on WDS performance assessment have been limited by the lack of data due to restricted access to buried infrastructure components. While the proposed approach focuses on WDSs, it can be adapted and applied to other types of infrastructure networks, such as gas, oil, and power networks, given appropriate assumptions on component operations and network flow. Significant research advances have been made on analyzing the performance of WDSs. However, existing modeling approaches present three main gaps in (i) the performance evaluation, (ii) the hazard consideration, and (iii) the uncertainty quantification, that this research is addressing.

First, existing studies have evaluated the performance of WDSs at either the component-level or system-level separately [6]. At the system level, Wang and O'Rourke [7] simulate the response of the WDS under seismic hazard where system serviceability is defined as the ratio of satisfied demand after the earthquake to total demand before the earthquake. Another study uses a connectivity-based model to evaluate the seismic vulnerability of WDS based on Monte Carlo simulation (MCS) and a shortest-path algorithm [8]. Wang et al. [9] propose the system serviceability index to evaluate the probabilistic performance of WDSs using MCS. At the component level, Shuang et al. [10] propose a

* Corresponding author.
E-mail address: hiba.baroud@vanderbilt.edu (H. Baroud).

https://doi.org/10.1016/j.ress.2021.107735
Received 28 July 2020; Received in revised form 31 March 2021; Accepted 29 April 2021
Available online 9 June 2021

model to evaluate the nodal vulnerability of WDS based on topological connectivity loss under cascading failures due to intentional attacks.

Second, most of the studies consider earthquake and intentional attacks with fewer research studies focusing on flood hazard in the mathematical modeling of the performance of WDSs, even though floods have caused more damage and fatalities than any other natural hazard in recent years [11]. Current performance analyses of WDSs under floods are based on HAZUS-MH[1] [13]. However, damage to buried pipes is typically not considered in HAZUS-MH since it is assumed that submergence of these pipes cannot occur [12]. This assumption can be invalid as reports on the long-term recovery efforts in the wake of Hurricane Katrina have shown damaged pipe infrastructure in New Orleans for drinking water and wastewater. This finding contradicts the typical risk analysis assumption that floods do not damage buried CISs [14] and highlights the importance of accurately evaluating infrastructure performance after the disruption.

The third and most significant challenge in evaluating the performance of WDSs is the lack of data to estimate parameters such as the component damage state and recovery rate. As a result, there exists uncertainty about the component vulnerability, network topology, and system serviceability of WDSs after a disruption. Uncertainty, a concept that reflects the lack of confidence, can be categorized as either *aleatory* or *epistemic*. Aleatory uncertainty, which stems from natural variability, cannot be reduced. In contrast, epistemic uncertainty, which is derived from the lack of knowledge, can be reduced to improve the model accuracy [15]. Failing to account for the epistemic uncertainty could lead to biased estimates of the system state, prolonging the recovery process. It is, therefore, critical to characterize the uncertainty in the assessment of the serviceability of disrupted infrastructure systems. Epistemic uncertainty can be quantified using different approaches such as interval analysis, Bayesian probability, and evidence theory [15]. Prior studies employing Bayesian approaches have primarily focused on predicting component failure [16,17]. *Bayesian networks* (BNs) have been used to predict pipe breaks [18] and have been converted from a fault tree model to estimate the probability of a water pipe being targeted by third-party activities [17]. Other approaches integrate Bayesian model averaging and Bayesian proportional hazard model to predict the failure of water mains [16]. However, little work has been conducted to assess the system-level serviceability of WDS under uncertainty using Bayesian approaches. Although BNs have been applied to the vulnerability assessment of other engineering systems [19,20], leveraging BNs to assess the serviceability of WDSs with limited data is challenging, particularly for large-scale WDSs. This is due to the lack of information on (i) the direction of edges in the *directed acyclic graph* (DAG) that represents the WDS and (ii) the *conditional probability table* (CPT) associated with each parent node in the DAG.

In summary, most of the existing approaches evaluate component- and system-level performance separately. Bayesian approaches have been successful at capturing uncertainty of component fragility. However, system-level approaches rarely consider the uncertainty in component-level estimations. Therefore, we propose an approach that explicitly takes into consideration uncertainty in the combined assessment of component vulnerability and system serviceability by integrating a hierarchical Bayesian model of network component fragility into the evaluation of system-level performance of WDSs using MCS and the shortest-path algorithm. Hierarchical Bayesian Models (HBMs) offer advantages in data-scarce situations. The models are able to integrate information from various sources and adapt to the structure of data, thereby reducing the variance of estimates [21] and addressing the challenge of specifying a prior distribution with limited data [22]. HBMs have been widely applied to risk and reliability analysis of different engineering systems [22–24]. In particular, Yan and Haimes [22] demonstrated the ability of HBMs to improve estimate accuracy through "*strength borrowing*" by pooling data from similar and related systems and applying HBMs to handle the lack of data in risk-based system analysis.

This research improves the state-of-the-art in the performance assessment of CISs by making the following contributions:

1. An approach where both epistemic uncertainty and aleatory uncertainty about the component failure probability are modeled. Epistemic uncertainty is rarely taken into account in prior studies that use MCS [25] or entropy-based methods [26,27] to analyze the vulnerability and reliability of WDSs under uncertainty. This study models the epistemic uncertainty using Bayesian updating of parameters and their distributions.
2. A method founded in the *hierarchical Bayesian model* (HBM) to address challenges of data scarcity, leverage additional data, and update the probabilistic evaluation of infrastructure performance. While HBM has been widely used in risk and reliability analysis, few studies handle the combination of epistemic and aleatory uncertainty which is frequently encountered in infrastructure performance modeling.
3. A method to incorporate Bayesian updating of fragility formulations of damage to infrastructure components under earthquake and flood hazards. Updated component fragility is integrated into the serviceability assessment of infrastructure systems.

The rest of this paper is organized as follows. Section 2 introduces the methodology, including the hierarchical Bayesian models, component failure estimation methods, and the proposed integrated approach for evaluating network serviceability based on MCS, and Section 3 describes the case study of the WDS in Shelby County, Tennessee, with the results presented in Section 4. Finally, Section 5 provides concluding remarks and discussions of future work.

2. Methodology

This section presents the methods that comprise the proposed approach with a focus on WDSs. The section starts with an overview of Bayesian methods (Section 2.1), followed by a description of component damage assessment (Section 2.2) that has been adapted in this study using HBM to account for uncertainty (Section 2.2.1), and ends with a description of the proposed framework integrating all these methods (Section 2.3).

The following notations are used in this research.

a	Regression coefficient in the formula for calculating repair rate.
b	Correlation distance.
c	A generic network component.
ds_i	Damage state i, $i = 1, \ldots, 5$.
g	Gravitational acceleration.
h_f	Standing water depth.
m	Number of segments in a pipe segment.
n	Number of pipe breaks within a segment.
s	Network serviceability.
w_c	Importance of a component to the network serviceability.
z_n	Binary variable indicating the functionality of a demand node.

[1] HAZUS-MH is a nationally applicable, standardized methodology provided by the U.S. Federal Emergency Management Agency (FEMA) estimate the potential loss from multiple types of hazards (earthquakes, floods, hurricanes, and tsunamis), and visualize the impact of such hazards [12].

F_{S_0}	Probability distribution of the network serviceability when all components are functional.
F_{S_c}	Probability distribution of the network serviceability when component c is removed.
I_c	Intensity of a hazardous event at the site of component c.
K	Scaling parameter for calculating repair rate.
M_w	Magnitude of an earthquake.
N_d	Number of demand nodes.
P_l	Failure probability of a pipe (link).
P_n	Failure probability of a node.
PGV	Peak ground velocity.
PGA	Peak ground acceleration.
RR	Repair rate of a pipe per 1000 ft.
R	Distance to the epicenter.
μ, σ	Mean and standard deviation of a normal distribution.
λ, ζ	Mean and standard deviation of the underlying normal distribution of a log-normal variable.
ϕ	Hyperparameters.
θ	Parameters of interest.
D	Data.
ΔL_i	Length of pipe segment L_i.

2.1. BayesIan updating and hierarchical Bayesian model

A Bayesian approach follows Bayes' theorem to update the estimate of the parameters of interest. Given a prior distribution of parameters (variables), $p(\theta)$, and a data likelihood function, $p(D|\theta)$, the posterior density, $p(\theta|D)$, is given by Eq. (1).

$$p(\theta|D) = \frac{p(\theta)p(D|\theta)}{p(D)} \propto p(\theta)p(D|\theta) \tag{1}$$

A Bayesian model is dynamically updated where the prior distribution is iteratively updated with the informative posterior distribution obtained using existing data as new data become available.

Bayesian approaches have been criticized for the potential subjectivity in specifying the priors when the physical basis or scientific model to justify the prior distribution is lacking [28]. When data is limited, HBM alleviates the subjectivity in assigning the prior distributions. Specifically, HBMs take into account the uncertainty around the parameters of the prior distribution by adding another layer of Bayesian inference. Instead of assigning a point value to the distribution parameters of θ, a hyperprior, represented by ϕ, is used to quantify the uncertainty around θ. According to the marginal posterior of ϕ shown in Eq. (3), ϕ is now partially dependent on the data rather than being an assumed value [22].

$$p(\theta, \phi|D) \propto \underbrace{p(D|\theta)}_{\text{likelihood}} \underbrace{p(\theta|\phi)}_{\text{prior}} \underbrace{P(\phi)}_{\text{hyperprior}} \tag{2}$$

$$p(\phi|D) = \int p(\theta, \phi|D)d\theta \propto \int p(D|\theta)p(\theta|\phi)P(\phi)d\theta \tag{3}$$

Since Eq. (2) rarely has a closed-form solution, simulation techniques are typically leveraged to generate samples of the posterior distributions of interest. Markov Chain Monte Carlo (MCMC) methods such as the Metropolis–Hastings algorithm, Gibbs sampling, and Hamilton Monte Carlo (HMC) have been developed to perform sampling efficiently [29,30].

2.2. Component damage assessment

This section describes the data, parameters, and models used to evaluate the damage at each WDS component under earthquake and flood hazards. To measure the impact of a hazard (I_c), the repair ratio (RR) is used for pipelines (links), and fragility curves are used for facilities (nodes). The probability of node failure is directly evaluated using fragility curves and the simulated hazard intensity (I_c). However, the probability of link failure requires the estimation of RR as an input (Section 2.2.3). To evaluate RR, prior studies have adopted a linear regression model as a function of hazard intensity (I_c) with deterministic coefficients estimated using a small sample of data from historical events. We propose to adapt this approach and use HBM to calculate RR such that the epistemic uncertainty in the estimated coefficients and the aleatory uncertainty in the hazard intensity are addressed. The details of Bayesian updating for RR are provided in Section 2.2.1 and the process of hazard simulation is provided in Section 2.2.2.

2.2.1. Repair ratio estimation using HBM

The repair ratio, which is calculated as the ratio between the number of repairs to a unit length of pipe, is commonly used as the indicator for the impact of seismic hazard on pipelines [3]. In this study, the seismic fragility model from the American Lifelines Alliance (ALA) [31] is adapted to a more general form shown in Eq. (4) in order to model multiple types of hazards. For earthquake hazard, historical data collected from records of repairs to service lines and water mains after recorded seismic intensities are generally used to fit a regression model to estimate RR (per 1000 ft of pipe length) as a function of hazard intensity I_c at the site of a component. For seismic intensity, PGV (in/s) is typically used. Due to the inherent variability of seismic intensity, there exists aleatory uncertainty about PGV which is represented by a random residual term, Eq. (8). Therefore, PGV is assumed to be a random variable. Of the collected data, pipe material, pipe joint type, pipe diameter, and soil condition also impact the measured RR values, so a fragility curve modification factor K is defined to scale the RR obtained from the regression model (Eq. (4)). HAZUS adopts the linear model from ALA to estimate the damage to water distribution systems given a seismic intensity from a specific earthquake scenario [32].

$$RR = aKI_c \tag{4}$$

In Eq. (4), a is the regression parameter and I_c is the intensity of the event. The factor K was originally developed for seismic events and is assumed here to be applicable to flood hazard as well.

To reflect flood intensity, a random variable h_f, measured in units of feet, represents the standing water depth in a certain location and will reflect I_c in Eq. (4). Historically, HAZUS provides floodplain extent and utilizes flood depth to calculate the damage to above-ground components such as pumping stations; however, recent studies document HAZUS missing as much as 75% of flooded areas when validating the predicted given actual flood extent of historical events [33]. The accuracy of this methodology depends on the accuracy of the flood depth estimates, which is largely determined by the quality of data that can be collected in the future. Ideally, repair records after major flood events should be collected and analyzed similarly to the existing methodology for earthquakes to obtain more accurate values of a and K through regression analysis and calculate the expected RR from flood events. With no database of records in existence yet, the initial values for a and K are adjusted from earthquake scenarios for floods, and the Bayesian updating accounts for uncertainty due to the lack of data.

The RR calculated from Eq. (4) is one of the main parameters used to estimate the probability of pipe failure. However, Eq. (4) is fit from a relatively small sample of data points on earthquake events. Additionally, there is no available data about pipe failures after flood events. The cost of collecting and analyzing such data is high due to sensitivity and security as well as the rare occurrence of disasters. Therefore, point values are often used for a and K even though the model itself has a poor fit, especially for large observed RR values [34].

To address this limitation, epistemic uncertainty is introduced to the coefficients a and K, and HBM is used to handle the epistemic uncertainty in estimating RR. In the HBM, a and K are assumed to be lognormal random variables with the respective uncertain means,

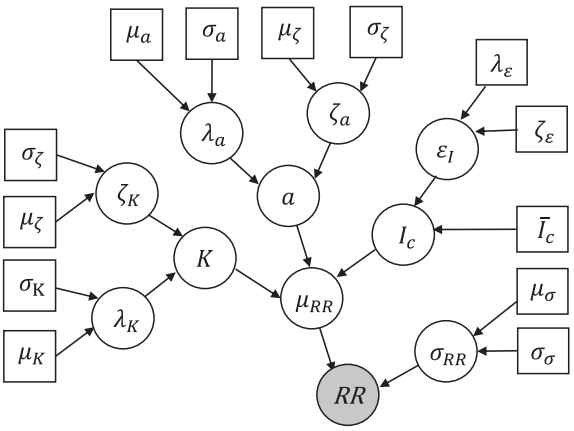

Fig. 1. HBM for estimating RR. Circles denote random variables. Squares denote constants. Shaded nodes denote observations while unshaded ones denote hidden variables/constants.

λ_a and λ_K, that follow a normal distribution. The standard deviations are assumed to be fixed at a relatively small value such that the normal distribution is weakly-informative [35]. When no prior information is available, the hyperpriors are typically assumed to be weakly-informative distributions to build a more robust model [36]. Note that the form of HBM is the same for the two hazards and the difference between the two hazards lies in the calculation of hazard intensity I_c. Modeling details of the hazard intensity I_c will be covered in Section 2.2.2. The HBM for estimating RR, visualized in Fig. 1 with the corresponding mathematical model given by Eq. (5), can be continuously updated with new pipe repair records to ensure the most accurate parameters are utilized to dynamically inform resource allocation during a disaster and for long-term resilience planning.

$$RR \sim \mathcal{N}\left(\mu_{RR}, \sigma_{RR}\right) \tag{5a}$$
$$\sigma_{RR} \sim \mathcal{N}\left(\mu_\sigma, \sigma_\sigma\right) \tag{5b}$$
$$\mu_{RR} = aKI_c \tag{5c}$$
$$\ln a \sim \mathcal{N}\left(\lambda_a, \zeta_a\right),\ \ln K \sim \mathcal{N}\left(\lambda_K, \zeta_K\right) \tag{5d}$$
$$\ln I_c = \ln \bar{I}_c + \ln \varepsilon_I,\ \ln \varepsilon_I \sim \mathcal{N}\left(\lambda_\varepsilon, \zeta_\varepsilon\right) \tag{5e}$$
$$\lambda_a \sim \mathcal{N}\left(\mu_a, \sigma_a\right),\ \lambda_K \sim \mathcal{N}\left(\mu_K, \sigma_K\right) \tag{5f}$$
$$\zeta_a \sim \mathcal{N}\left(\mu_\zeta, \sigma_\zeta\right),\ \zeta_K \sim \mathcal{N}\left(\mu_\zeta, \sigma_\zeta\right) \tag{5g}$$

2.2.2. Hazard intensity

The variable I_c from Eq. (4) must be determined for each component of the network to calculate individual failure probabilities. Due to the natural variability, there exists aleatory uncertainty around the hazard intensity.

For earthquake scenarios, the hazard intensity I_c can be measured in terms of peak ground velocity PGV (cm/s) or peak ground acceleration PGA (cm/s^2). PGA and PGV are estimated from their respective attenuation equation that models seismic intensity at a site from an earthquake of magnitude M_w and distance from the epicenter R (km). The attenuation equations for the median PGV and PGA adopted in previous research are shown in Eqs. (6) and (7) [8,34].

$$\log_{10}(\overline{PGA}) = 3.79 + 0.298 \times (M_w - 6) - 0.0536 \times (M_w - 6)^2 - \log_{10}(R) - 0.00135 \times R \tag{6}$$

$$\log_{10}(\overline{PGV}) = 2.01 + 0.422 \times (M_w - 6) - 0.0373 \times (M_w - 6)^2 - \log_{10}(R) \tag{7}$$

The median seismic intensity PGV from Eq. (7) is used to describe the damage to pipes (link components) while the median PGA from Eq. (6) is used to describe damage to facilities (node components). The standard deviations of the residuals associated with Eqs. (6) and (7) to capture the aleatory uncertainty around seismic intensities are typically assumed to be a lognormal distribution with a median value equal to 1.0 and a standard deviation of 60% [8]. The intensity of a seismic event varies across the system and is usually modeled as a homogeneous two-dimensional stochastic field with a residual term [37]. The estimation equation for the logarithmic residual of the seismic intensity ($\overline{PGA}$ or $\overline{PGV}$) at the site of a component c, denoted by $\ln I_c$, is given by Eq. (8) where $\bar{I}_c$ represents the mean value of I_c. In order to account for the correlation between neighboring nodes and its influence on the failure probability, an autocorrelation function of logarithmic residuals is used for the seismic intensities at the site of components c_i and c_j. In Eq. (9), R_c refers to the distance from the site of component c to the epicenter, the correlation distance b is the strength of the spatial correlation and is typically assumed to be 30 km [37].

$$\ln(\varepsilon_I) = \ln\left(\frac{I_c}{\bar{I}_c}\right) \tag{8}$$

$$\rho(\ln I_{c_i}, \ln I_{c_j}) = \exp\left(-\frac{\|R_{c_i} - R_{c_j}\|}{b}\right) \tag{9}$$

The flood intensity is measured by flood depth (feet) estimated based on the digital elevation model (DEM). The elevation of a given location is subtracted from the maximum water surface elevation along the cross-section of a flood basin. However, due to the slope of the floodplain and the complexity in flow paths, estimating flood depth using cross-section maximum flood water elevation is challenging [38]. A more accurate method to generate spatially-explicit floodwater depth is through numerical simulation given data on the hydrological characteristics and river morphology [38]. A commonly used hydrology-based flood map application is FEMA HAZUS Flood Maps [12]. The HAZUS Flood Model uses characteristics such as frequency, discharge, and ground elevation to model the spatial variation in flood depth and velocity. In this study, we adopt the simulation-based methodology using HAZUS. It is important to note that HAZUS can underestimate the flood depths by considering the precipitation in the study region without accounting for cascading effects from upstream rivers. To offset the underestimation, a longer return period can be considered in HAZUS so that the simulated flood depths are approximate to observations at the gauges within the study area. The HAZUS Flood Model is subject to several sources of uncertainty, such as the variation in channel and floodplain elevation in the Digital Elevation Model (DEMs) and the variation in floodplain extent and depth in the River Hydraulic Model [39]. To characterize the resulting uncertainty around the flood depths, a 50% standard deviation is assumed for estimates of flood depths. To improve the accuracy of these estimates, the average of the estimates from two simulations can be used. If the flood depth estimates at some components of the WDS are missing in one simulation due to the removal of problematic reaches, the estimates from the second simulation can be used. If the missing values from the two simulations overlap (i.e., the data for these reaches are not available in HAZUS), the mean of the estimates derived from elevation-based interpolation can be used.

2.2.3. Failure probability

A WDS is represented by a network consisting of nodes and links. Given the hazard intensity and RR estimates, a failure probability is derived for each node and link in the WDS.

Node Failure. The physical damage to facilities in a WDS such as elevated storage tanks or pumping stations is described using fragility curves used in HAZUS [32]. A total of five damage states are defined, including none (ds_1), minor (ds_2), moderate (ds_3), extensive (ds_4), and complete (ds_5). As an example, the fragility curve for above-ground steel tank entering different damage states is shown in Fig. 2. In this study, damage state ds_5 is adopted.

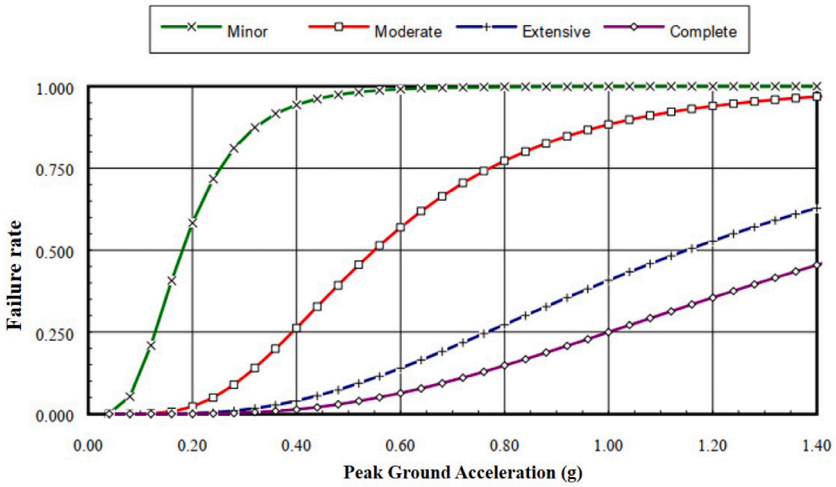

Fig. 2. Fragility curve for above-ground steel tank under earthquake hazard [32]. Failure rate represents the probability of a component reaching a specific damage state given PGA.

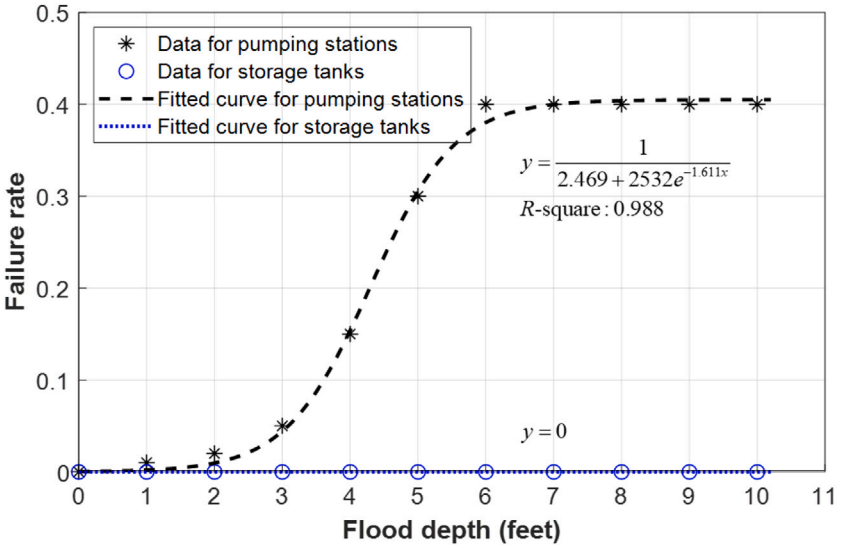

Fig. 3. Fragility curve for water facilities under flood hazard.

The seismic fragility curve is described with a log-normal distribution as a function of PGA given in Eq. (10) where P_n describes the failure probability of each node, λ_{PGA} represents the logarithmic mean of PGA that is measured in the gravitational acceleration g, ζ_{PGA} describes the standard deviation of $\ln(PGA)$, and $\phi(\cdot)$ is the standard normal cumulative distribution function.

$$P_n(PGA) = \phi\left(\frac{\ln(PGA) - \lambda_{PGA}}{\zeta_{PGA}}\right) \tag{10}$$

The intensity of a flood event is described by the flood depth. Flood fragility curves given the flood depth are typically derived from historical data, damage survey data, or expert opinions [40]. Since fragility curves of water facilities are not available in the literature, historical data of the pumping stations (medium/large, above ground) and storage tanks (all, above ground) from the HAZUS Flood Model technical manual [12] are leveraged to fit the fragility curves presented in Fig. 3. The two curves are used to evaluate the failure probability of water facilities in the case study of Shelby County, TN. Note that the failure probability of the elevated storage tanks is always 0 when the flood depth is under 10 ft. For other types of pumping stations or storage tanks, the fragility curves can be derived in the same manner.

Link Failure. Since the hazard intensity, PGV or flood depth, varies along a pipe, the pipe is assumed to be equally divided into m segments and the repair ratio RR_i is used to represent the rate at which a pipe breaks. A Poisson distribution is used to model the number of breaks for each segment where n is a random variable denoting the number of times a pipe segment breaks, RR_i is the rate at which this event occurs, and ΔL_i is the pipe segment length, Eq. (11). Setting $k = 0$ results in the probability that the segment is functioning. Since the failure of one segment results in the failure of the entire pipeline, then the probability that a pipe (link) fails, P_l, is the complementary of the probability that none of the segments in that pipeline fail evaluated by multiplying $P_{L_i}[n = 0]$ for all m segments, Eq. (12) [34].

$$P_{L_i}[n = k] = \exp\left(-RR_i \times \Delta L_i\right) \times \frac{(RR_i \times \Delta L_i)^k}{k!} \tag{11}$$

$$P_l = 1 - \exp\left(-\sum_{i=1}^{m} RR_i \times \Delta L_i\right) \tag{12}$$

2.3. Integrated approach for assessing network serviceability

In order to evaluate the serviceability of a water distribution network under hazard uncertainty, we build a double-loop MCS to consider multiple disruption scenarios and integrate the uncertainty from component damage assessment in the network model and simulation

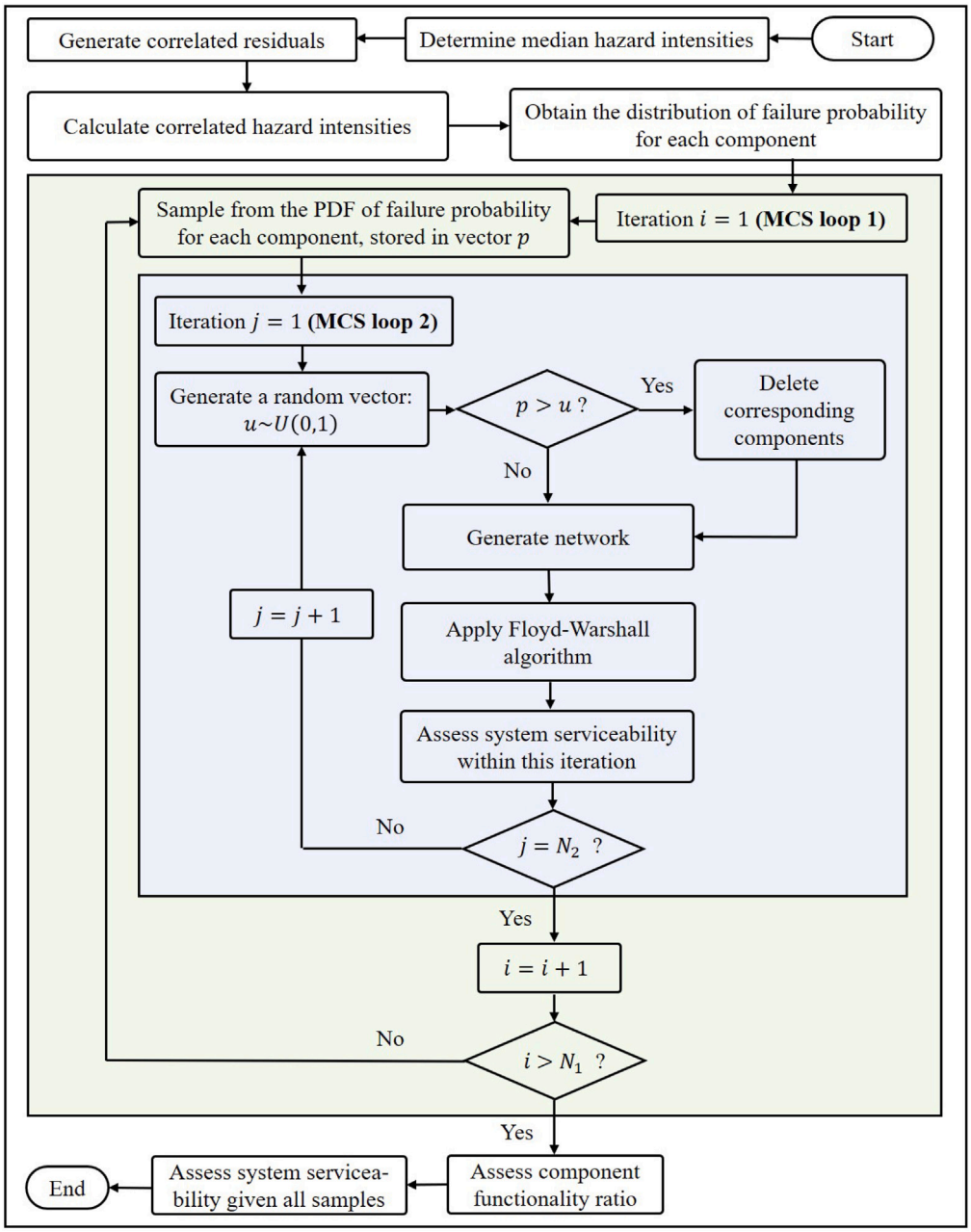

Fig. 4. Flowchart of the proposed approach.

for assessing network serviceability. The hierarchical Bayesian model is at the core of modeling component failure and the simulation captures epistemic uncertainty in the evaluation of network serviceability. The approach is illustrated in Fig. 4 and follows 9 steps. In step 6, the relationships between nodes is considered directional (dependency) instead of bidirectional (interdependency). Therefore, the serviceability assessment considers the dependence of child nodes on the respective parent node, e.g., distribution nodes/relay nodes (demand nodes) on the storage tanks (supply nodes). When the epistemic uncertainty is introduced in step 7, a distribution of the serviceability of the network is generated rather than a single point estimate of the average serviceability described in Eq. (13). This distribution allows for an understanding of the impact of uncertain model parameters on the outcome of disruption scenarios.

1. The natural hazard scenario is generated. For the earthquake hazard, the epicenter and magnitude of the earthquake are defined. For the flood hazard, the severity of the event based on the return period, such as a 100-year or 200-year flood event, is determined.
2. The intensity of the natural hazard, i.e. PGA or PGV for earthquake or the standing water depth for flood at the location of vulnerable network components, is estimated respectively.
3. A random vector of correlated hazard intensities for each component is generated.
4. The probability of failure for each component of the network is calculated. HBM is used to obtain the component failure probability. For simplicity, the components are assumed to be either fully functional or inoperable.
5. The status of a component under the hazard scenario is determined by comparing its failure probability to a random number $r \sim U(0,1)$. If the failure probability is greater than r, then the component is considered damaged and is removed from the network and a subgraph of the original network is generated.

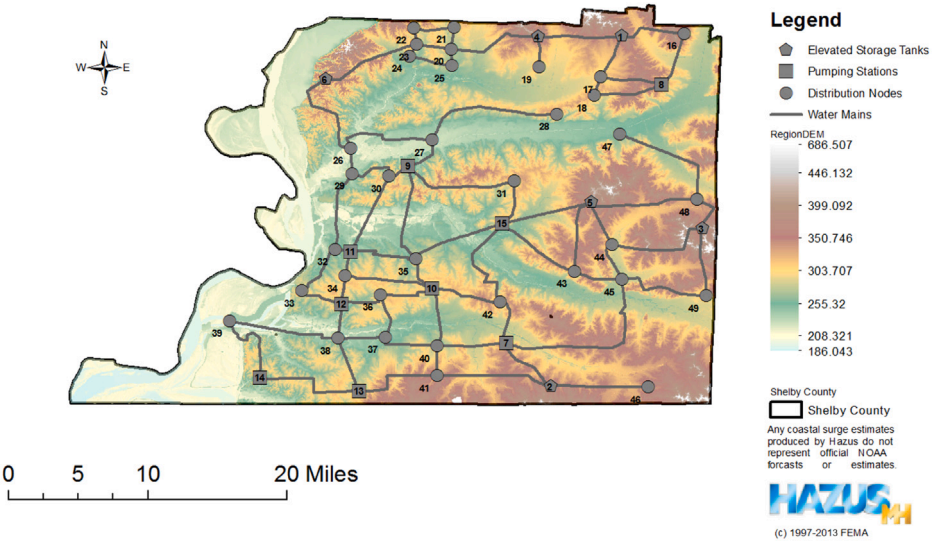

Fig. 5. WDS of Shelby County [12].

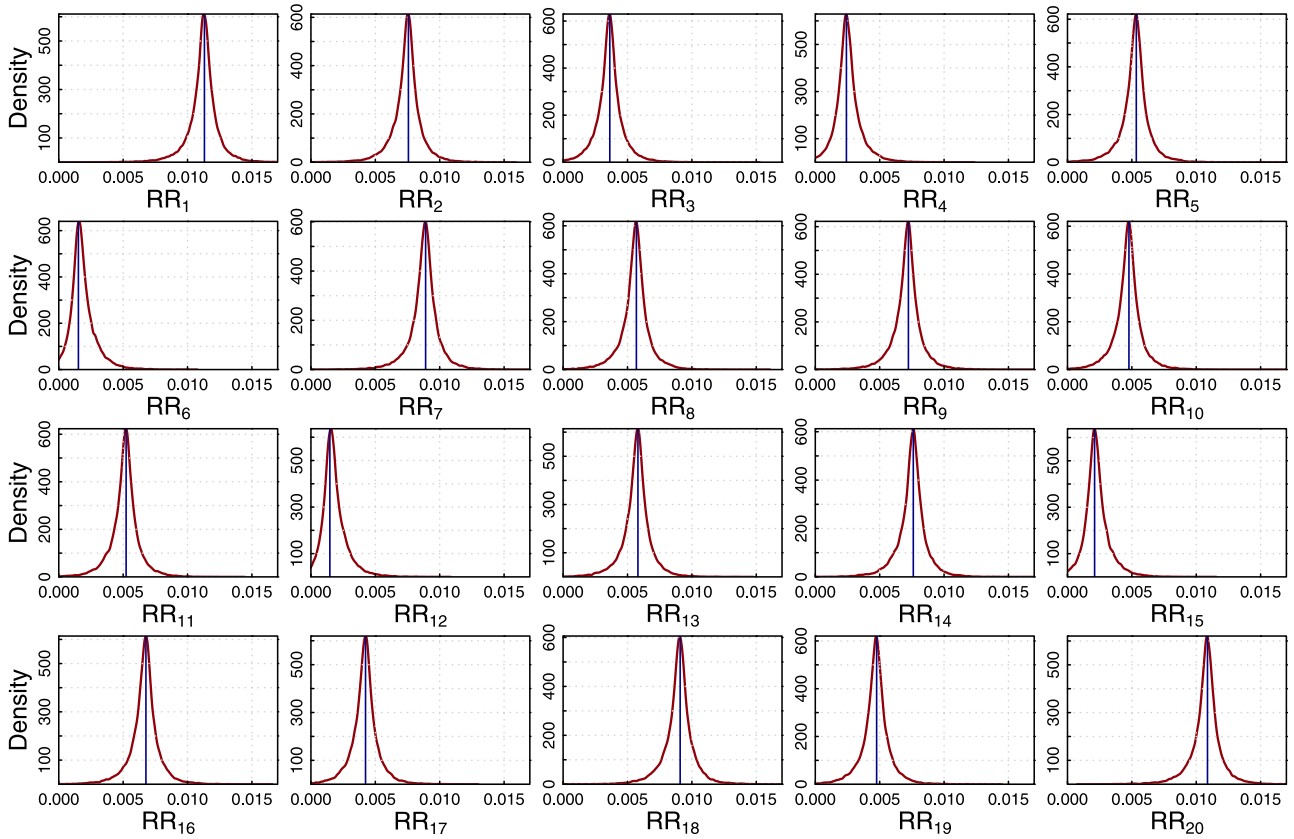

Fig. 6. Comparison between the predictive posterior of RR (red curve) and 20 observations of RR (blue vertical line).

6. The functionality of components and network serviceability are evaluated using the Floyd–Warshall algorithm [41], which finds the shortest path between all pairs of nodes simultaneously. In this algorithm, the distance between disconnected nodes is equal to infinity. If at least one path exists from a demand node to a source node, the demand node is considered to be functional.
7. Steps 3–6 are performed N_2 times to develop a probability distribution of component functionality and the network serviceability.
8. Steps 3–7 are repeated for N_1 times to capture the uncertainty in system serviceability due to the epistemic uncertainty associated with a and K.

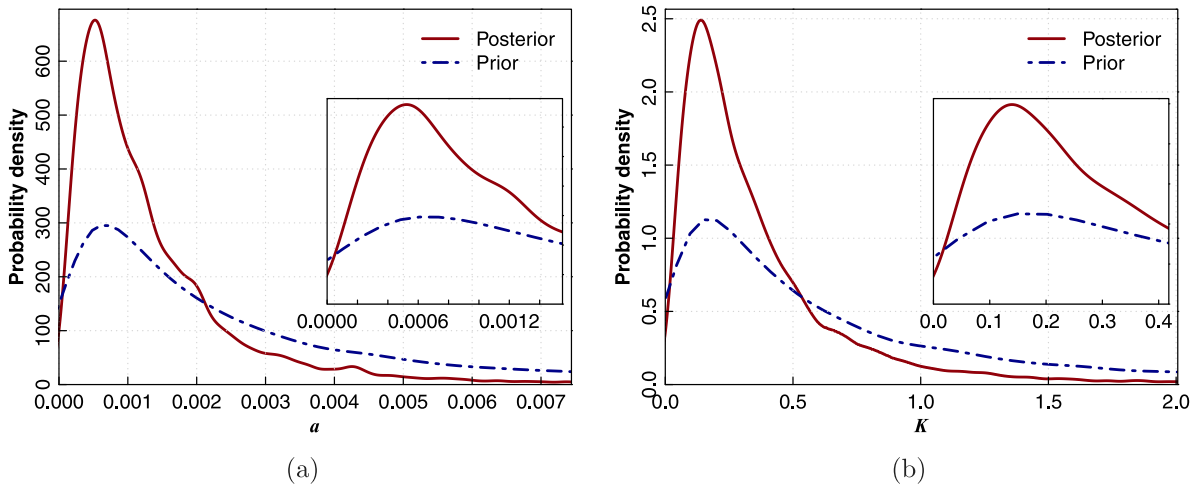

Fig. 7. Uncertainty quantification of (a) a and (b) K using HBM.

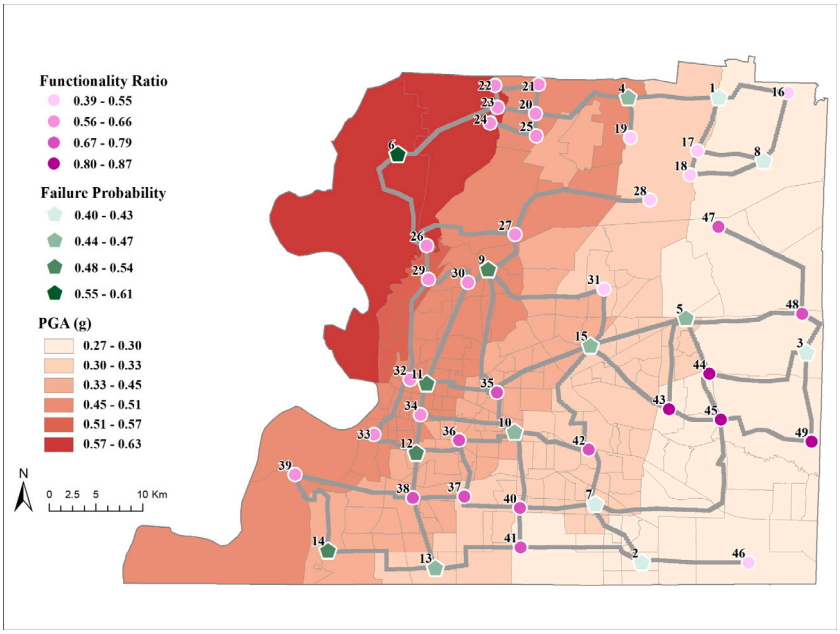

Fig. 8. Functionality of relay node and failure probability of storage tanks and pumping station along with the median PGA.

9. Once the functionality ratio of the demand nodes is obtained, network serviceability, s, is evaluated using Eq. (13) where $z_{n_i} \in \{0, 1\}$ with $z_{n_i} = 1$ indicating that demand node i is functional; N_d is the total number of demand nodes.

$$s = \frac{\sum_{i=1}^{N_d} z_{n_i}}{N_d}, \; s \in [0, 1] \tag{13}$$

3. Case study

3.1. Network description

To illustrate the proposed approach, a case study of a real-world WDS in Shelby County [42], Tennessee is presented in this section. The WDS (Fig. 5) serves approximately one million people. The network consists of 6 elevated storage tanks, 9 pumping stations, 34 relay nodes, and 71 buried water pipes. The relay nodes are the demand nodes while the storage tanks are the supply nodes. Since the relay nodes constitute the branch points where the water pipes intersect, the damage to these nodes is not considered in this study. The pipes installed before 1975 were made from cast iron with molten lead joints (before 1959) or mechanical joints (1959–1975) while the pipes installed after 1975 were made from ductile iron pipes with slip joints. The pipe diameter ranges from 6 inches to 48 inches [8].

3.2. Natural hazard scenario

3.2.1. Earthquake

The study area is earthquake-prone because the New Madrid Seismic Zone is centered northwest to Shelby County. The maximum probable earthquake with an exceedance probability of 2% in 50 years centers at 35.3 N and 90.3 W [43]. The distance of the WDS components to the epicenter of the maximum probable earthquake ranges from 20 km to 65 km, with a mean value of approximately 40 km. Once the earthquake scenario is defined, the median PGA at a point is solely dependent on the distance to the epicenter. Therefore, the median PGA contours in Shelby County with the default data in HAZUS given the earthquake scenario above show a rippling shape (Fig. 8), decreasing

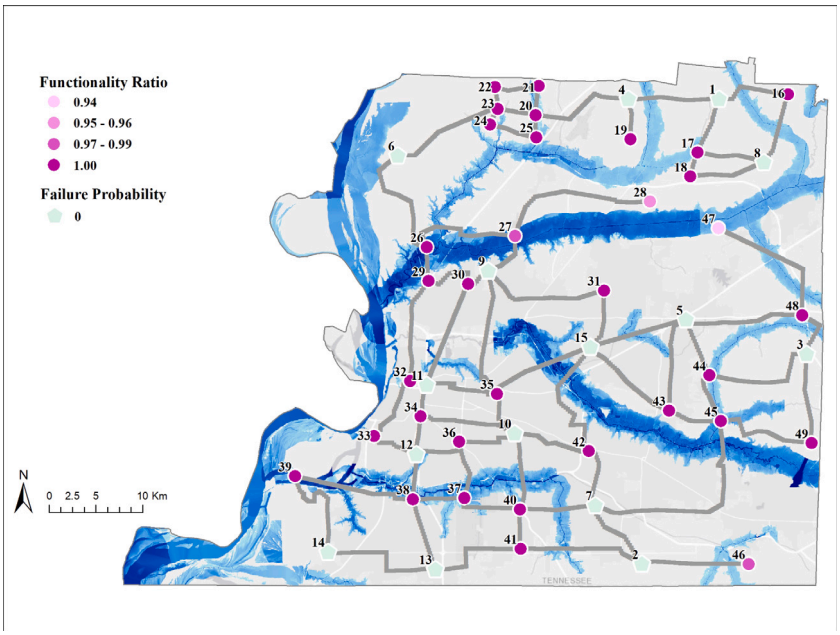

Fig. 9. Failure probability of water distribution facility and functionality ratio of relay nodes under flood (The blue area is the flood zone).

gradually from the highest value of approximately 0.6 in the northwest corner to the lowest value of around 0.3 in the southeast corner.

3.2.2. Flood hazard scenario

The Mississippi River and several smaller rivers run through Shelby County, making the area particularly vulnerable to flooding. The blue area in Fig. 9 shows the 100-year HAZUS-derived flood zone. In order to simulate the 2011 flood event, a 1000-year flood is simulated in HAZUS based on historical records of river crests in Memphis [44],

3.3. Experiment setup

For damage caused by earthquakes and a damage state ds_5, λ_{PGA} =ln(1.5) is used for both water storage tanks and pumping stations, and $\zeta_{PGA} = 0.6$ is used for water storage tanks while $\zeta_{PGA} = 0.8$ is used for pumping stations [32]. The correlation distance b is set to 30 km for earthquakes whereas correlation is not considered in calculating the flood depth at different sites of network components.

In calculating the repair rate of water pipes under seismic activities, $\mu_{\lambda_K} = \ln(0.5)$ and $\mu_{\lambda_a} = \ln(0.00187)$ are assumed based on the point estimate $K = 0.5$ and $a = 0.00187$ from ALA. For the damage caused by flood, $\mu_{\lambda_K} = \ln(0.5)$ is also assumed and the coefficient μ_a is assumed to be $\ln(0.001)$ so that the magnitude of the failure probability of water pipes under flood is close to that under earthquake. Given no prior information, a generic weakly informative distribution [35], $\mathcal{N}(0,1)$, or a standard deviation of 1.0 is assigned to the prior or hyperprior distributions (Eq. (14) to Eq. (17)). These assumptions are crude due to the lack of data on RR under flood hazard. Once new data about RR become available, the assumptions can be modified to make the distributions more informative.

$$\sigma_{RR} \sim \mathcal{N}(0,1) \tag{14}$$

$$\ln \varepsilon_I \sim \mathcal{N}(0,1) \tag{15}$$

$$\lambda_a \sim \mathcal{N}\left(\mu_{\lambda_a}, 1\right),\ \lambda_K \sim \mathcal{N}\left(\mu_{\lambda_K}, 1\right) \tag{16}$$

$$\zeta_a \sim \mathcal{N}(0,1),\ \zeta_K \sim \mathcal{N}(0,1) \tag{17}$$

The proposed HBM is implemented with Stan, a probabilistic programming language that implements full Bayesian statistical inference [35]. The *No-U-Turn sampler* (NUTS) [45], a variant of HMC embedded in Stan, is leveraged to perform the sampling. This algorithm is much more efficient than classical MCMC algorithms, e.g. Metropolis–Hastings or Gibbs sampler. In performing the serviceability assessment, N_1 and N_2 are set to 1.0×10^3, therefore a total of 1.0×10^6 simulation runs are conducted to obtain the mean functionality ratio of each relay node under earthquake and flood hazard.

4. Results and discussion

4.1. Model fitness and parameter updating

To evaluate the fitness of the proposed HBM, we conduct the *posterior predictive check*, i.e., simulating data given the fitted model and comparing the replicated data to the observations [35]. The comparison between 20 observations of RR and the respective posterior predictive distribution is presented in Fig. 6. The mean of the posterior predictive distributions matches the respective observed values of RR, demonstrating the goodness of fit of the proposed model.

Further validation is presented in Fig. 7 by comparing the prior and posterior distributions of the regression coefficients, a and K, in the equation used for estimating the repair rate. The posterior distribution of a and K has lower variability and thinner tails, indicating reduced uncertainty about the coefficients after Bayesian updating. Note that the difference between the mode of the posterior (maximum a posteriori) and that of the prior for a or K is not significant because an informative prior, rather than a non-informative prior (e.g., the uniform distribution), has been used for each parameter.

4.2. Serviceability assessment

As the component fragility is distinct under earthquake and flood events, the distribution of functionality ratio under different hazards are disparate. Fig. 10 indicates that the functionality ratios of relay nodes are much higher under flood than under earthquake. Under seismic hazard, the functionality ratios range between 0.4 and 0.9 while under flood, most of the functionality ratios are close to 1.0. The reason is that the components are more vulnerable to seismic hazard than to flooding because during a flood event, components located at high altitude are not inundated (Fig. 9) while under an earthquake event, all the components are subject to the impact of seismic waves (Fig. 8). In particular, node 28 has a low functionality ratio under both hazards

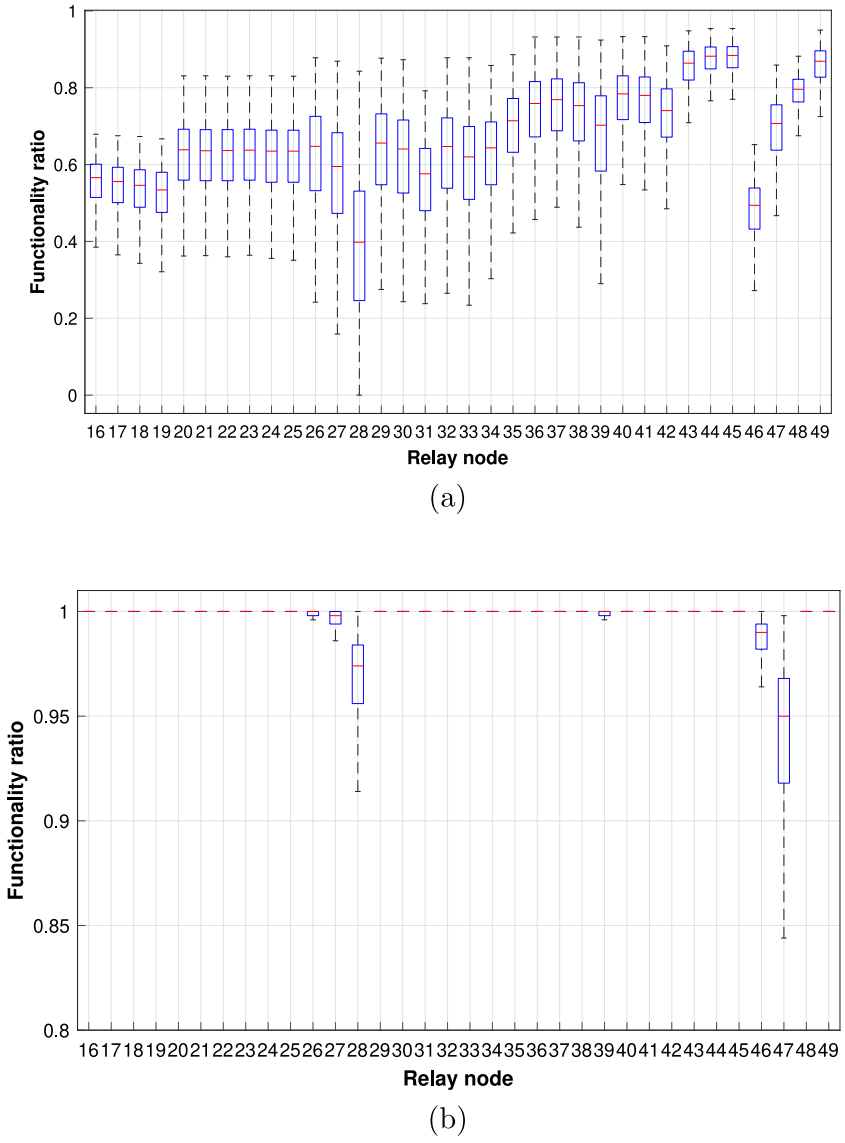

Fig. 10. Component functionality ratio under (a) earthquake and (b) flood.

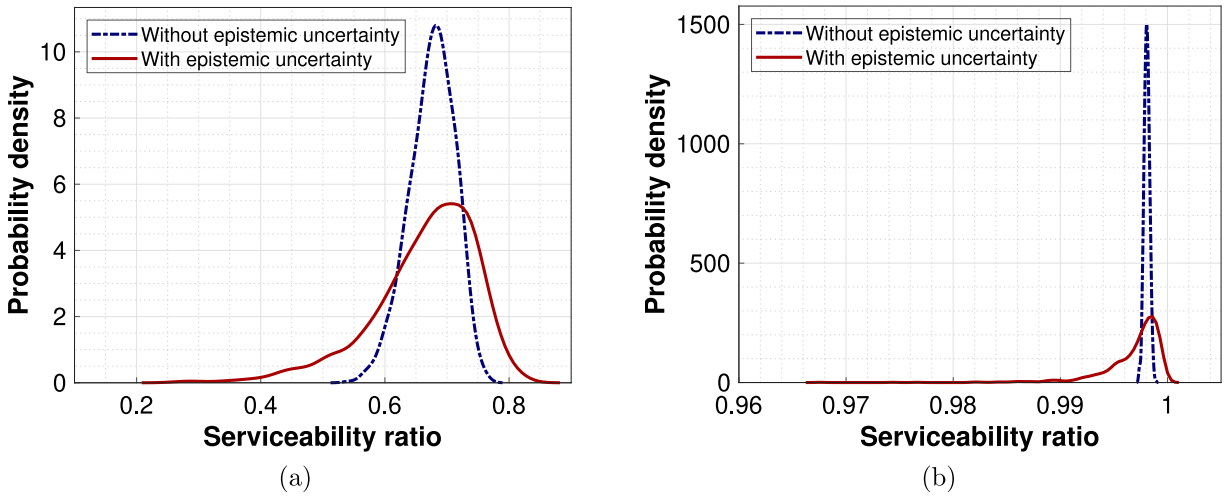

Fig. 11. PDF of the serviceability ratio under earthquake (a) and flood (b).

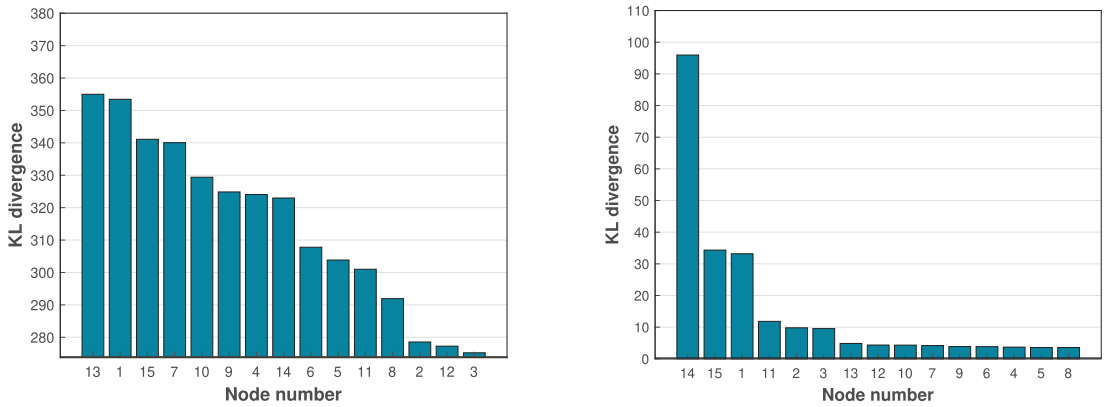

Fig. 12. Node importance under earthquake (a) and flood (b).

because it is only accessible from one water pipe and it is far from the water storage tanks. In comparison, node 46 and node 47 have higher functionality ratios because they are close to storage tanks. However, node 47 has the lowest functionality ratio under flood hazard because it is closely located to the river and it is accessible through only one water pipe. As such, node functionality is dependent on the fragility of nodes and the topology of the system. These observations indicate that system topology is more important in determining the functionality ratio under seismic hazard while component fragility is the dominant factor under flood hazard.

In order to evaluate the impact of considering epistemic uncertainty on the performance assessment, the serviceability PDFs with and without epistemic uncertainty are compared under earthquake and flood hazards, Fig. 11. Note that the aleatory uncertainty is always present and thus should not be removed because it is inherent to the hazard intensity. The comparison between the PDFs with epistemic uncertainty under earthquake and flood matches the results of the functionality ratio because the mean serviceability ratio is much higher under flood than under earthquake. The spread of the PDF under flood, irrespective of the uncertainty, is narrower when compared to that under earthquake. This small variability is due to the fact that only a small portion of components fail under flood, leading to a small number of different subgraphs constructed by removing inoperable nodes and links in the MCS.

The PDF of serviceability becomes wider after incorporating epistemic uncertainty. Using HBM to address epistemic uncertainty allows for an improved estimation of the serviceability of WDSs. This can help decision-makers design robust vulnerability reduction plans across a wide range of hazard scenarios [46].

4.3. Node importance analysis

Node importance analysis is a crucial step in infrastructure management as critical nodes functionality can significantly impact the serviceability of the entire network, thereby guiding decision-making on resource allocation and prioritization of repair activities when multiple nodes are disrupted [47]. To obtain the component importance ranking, a method based on Kullback–Leibler (KL) divergence is adopted, which is often used as a measure of dissimilarity between two probability distributions in information theory. The KL divergence from one discrete probability distribution, $Q(x)$, to another discrete probability distribution $P(x)$ defined on the same discrete probability space $\mathcal{X}$, is given by Eq. (18) [48].

$$D_{\mathrm{KL}}(P \parallel Q) = -\sum_{x \in \mathcal{X}} P(x) \log \frac{Q(x)}{P(x)} \tag{18}$$

The importance of a component c_i is defined to be the KL divergence from the probability distribution of the network serviceability, $F_{S_{c_i}}$, after removing c_i (i.e., when c_i is not functional or not hardened, hence vulnerable to failure) to the distribution of serviceability, F_{S_0}, when none of the components is removed (i.e., all components are functional). The importance of component i, denoted by w_{c_i}, can be computed according to Eq. (19).

$$w_{c_i} = D_{\mathrm{KL}}(F_{S_0} \parallel F_{S_{c_i}}) \tag{19}$$

Algorithm 1: Rank components based on KL divergence

1: Run the double-loop MCS to generate the initial distribution of system serviceability F_{S_0} given all components with the respective failure probability
2: **for** $i = 1$ to N **do**
3: Remove node i
4: Run the double-loop MCS to obtain the serviceability distribution S_{c_i}
5: Calculate component importance with Eq. Eq. (19)
6: **end for**
7: Sort w_{c_1} to w_{c_N} in descending order

When the importance of nodes that represent storage tanks and pumping stations is evaluated using MCS, each node is removed individually to reveal its contribution to the decrease in the network serviceability. The steps for ranking components based on KL divergence are summarized in Algorithm 1.

The results in Fig. 12 show that the ranking of node importance under earthquake is different from that under flood. Under earthquake, nodes 13 and 1 have the highest influence on the overall system serviceability while nodes 2, 12, and 3 have the least influence on the serviceability. Under flood hazard, node 14 is by far the most important to the system serviceability. Node 4 -10, 12 and 13 have a trivial impact on the serviceability.

5. Conclusion

This study presents a Bayesian updating framework integrated with Monte Carlo simulation and network algorithms to evaluate the performance of critical infrastructure under uncertainty of natural hazards. The uncertainty about component fragility due to data scarcity and hazard intensities is measured using a hierarchical Bayesian model. Then, the uncertainty is propagated to the system level using MCS to assess the network serviceability under the impact of different types of natural hazards. The proposed framework is illustrated with a case study of a real-world WDS in Shelby County, Tennessee. The results indicate that the WDS performs differently under different hazard scenarios. The network is more vulnerable to earthquake hazard than flood hazard. Further, component functionality is driven by network

topology under earthquake hazard whereas under flood hazard component vulnerability is more important. The difference is also reflected in the ranking of node importance under the two hazard scenarios. The ranking of components can be used by utility managers and emergency responders to inform the allocation of resources in disaster preparedness and response. The proposed approach leveraging HBM enables various considerations of infrastructure protection, such as modeling the correlation between multiple hazards (e.g., the impact of earthquake risk on flood hazard) [49] and the integration of vulnerability quantification into resilience planning frameworks [50].

Future work of this research include refining the model for estimating the failure probability of components under the flood hazard using available data, which can be collected from repair records or through the use of sensing technologies that provide real-time detection of pipe failures or leakages [51]. While the purpose of this study is to demonstrate how HBM can be leveraged to evaluate the serviceability under both aleatory and epistemic uncertainty, the current model does not take into account the hydraulic characteristics of the components of WDS. Future work would incorporate the pressure-driven or demand-driven hydraulic analysis to account for the various factors influencing WDS performance and improve the applicability of the proposed approach. Another direction for further research is to incorporate interdependencies among infrastructure systems into the Bayesian updating framework for assessing the serviceability given that WDSs are often coupled with power grids. For example, flooding caused by water pipe breaks can damage closely located power distribution facilities, which may cause the pumping stations to fail due to loss of power supply. As such, the interdependency-related failures must be included to provide a serviceability assessment of interdependent infrastructure systems.

CrediT authorship contribution statement

Jin-Zhu Yu: Methodology, Validation, Investigation, Formal analysis, Writing - original draft. **Mackenzie Whitman**: Writing - original draft, Literature review. **Amirhassan Kermanshah**: Data curation, Visualization, Formal analysis, Writing - original draft. **Hiba Baroud**: Conceptualization, Supervision, Writing - review & editing, Funding acquisition.

Declaration of competing interest

The authors declare that they have no known competing financial interests or personal relationships that could have appeared to influence the work reported in this paper.

Acknowledgments

This research was partially supported by the National Science Foundation through award no. 1635717. We would also like to thank Madeline Allen and Leslie Gillespie-Marthaler for their help with performing flood simulation using HAZUS, and William Sisson for sharing his expertise in the topological and operational attributes of the water distribution system in Shelby County.

References

[1] Ouyang M, Xu M, Zhang C, Huang S. Mitigating electric power system vulnerability to worst-case spatially localized attacks. Reliab Eng Syst Saf 2017;165:144–54.
[2] White House. Presidential policy directive: Critical infrastructure security and resilience. 2013.
[3] Laucelli D, Giustolisi O. Vulnerability assessment of water distribution networks under seismic actions. J Water Res Plann Manage 2014;141(6):04014082.
[4] Wisetjindawat W, Kermanshah A, Derrible S, Fujita M. Stochastic modeling of road system performance during multihazard events: flash floods and earthquakes. J Infrastruct Syst 2017;23(4):04017031.
[5] ASCE. 2017 infrastructure report: drinking water. American Society of Civil Engineers ASCE; 2017, p. 5, https://www.infrastructurereportcard.org/cat-item/drinking-water/.
[6] Pudasaini B, Shahandashti S. Identification of critical pipes for proactive resource-constrained seismic rehabilitation of water pipe networks. J Infrastruct Syst 2018;24(4):04018024.
[7] Wang Y, O'Rourke TD. Seismic Performance Evaluation of Water Supply Systems, vol. 15. Multidisciplinary Center for Earthquake Engineering Research Buffalo, NY; 2008.
[8] Adachi T, Ellingwood BR. Serviceability assessment of a municipal water system under spatially correlated seismic intensities. Comput-Aided Civ Infrastruct Eng 2009;24(4):237–48.
[9] Wang Y, Au S-K, Fu Q. Seismic risk assessment and mitigation of water supply systems. Earthq Spectra 2010;26(1):257–74.
[10] Shuang Q, Zhang M, Yuan Y. Node vulnerability of water distribution networks under cascading failures. Reliab Eng Syst Saf 2014;124:132–41.
[11] Kermanshah A, Derrible S, Berkelhammer M. Using climate models to estimate urban vulnerability to flash floods. J Appl Meteorol Climatol 2017;56(9):2637–50.
[12] Division FEMAM. Hazus-MH technical manual: flood model. Washington D.C.: Department of Homeland Security; 2013, https://www.fema.gov/media-library-data/20130726-1820-25045-8292/hzmh2_1_fl_tm.pdf.
[13] Nastev M, Todorov N. Hazus: A standardized methodology for flood risk assessment in Canada. Canad Water Res J 2013;38(3):223–31.
[14] Copeland C. Hurricane-damaged drinking water and wastewater facilities: impacts, needs, and response. Congressional Research Service, Library of Congress; 2005.
[15] Mullins J, Ling Y, Mahadevan S, Sun L, Strachan A. Separation of aleatory and epistemic uncertainty in probabilistic model validation. Reliab Eng Syst Saf 2016;147:49–59.
[16] Kabir G, Tesfamariam S, Sadiq R. Predicting water main failures using Bayesian model averaging and survival modelling approach. Reliab Eng Syst Saf 2015;142:498–514.
[17] Xiang W, Zhou W. Bayesian network model for predicting probability of third-party damage to underground pipelines and learning model parameters from incomplete datasets. Reliab Eng Syst Saf 2021;205:107262.
[18] Francis RA, Guikema SD, Henneman L. Bayesian belief networks for predicting drinking water distribution system pipe breaks. Reliab Eng Syst Saf 2014;130:1–11.
[19] Yodo N, Wang P, Zhou Z. Predictive resilience analysis of complex systems using dynamic Bayesian networks. IEEE Trans Reliab 2017;66(3):761–70.
[20] Khakzad N. Application of dynamic Bayesian network to risk analysis of domino effects in chemical infrastructures. Reliab Eng Syst Saf 2015;138:263–72.
[21] Gelman A, Carlin JB, Stern HS, Dunson DB, Vehtari A, Rubin DB. Bayesian data analysis. Chapman and Hall/CRC; 2013.
[22] Yan Z, Haimes YY. Cross-classified hierarchical Bayesian models for risk-based analysis of complex systems under sparse data. Reliab Eng Syst Saf 2010;95(7):764–76.
[23] Yu H, Khan F, Veitch B. A flexible hierarchical Bayesian modeling technique for risk analysis of major accidents. Risk Anal 2017;37(9):1668–82.
[24] Yu J-Z, Baroud H. Quantifying community resilience using hierarchical Bayesian kernel methods: A case study on recovery from power outages. Risk Anal 2019;39(9):1930–48.
[25] Fragiadakis M, Christodoulou SE. Seismic reliability assessment of urban water networks. Earthq Eng Struct Dynam 2014;43(3):357–74.
[26] Wang F, Zheng X-z, Li N, Shen X. Systemic vulnerability assessment of urban water distribution networks considering failure scenario uncertainty. Int J Crit Infrastruct Prot 2019;26:100299.
[27] Emamjomeh H, Jazany RA, Kayhani H, Hajirasouliha I, Bazargan-Lari MR. Reliability of water distribution networks subjected to seismic hazard: Application of an improved entropy function. Reliab Eng Syst Saf 2020;197:106828.
[28] Gelman A. Objections to Bayesian statistics. Bayesian Anal 2008;3(3):445–9.
[29] Beck JL, Au S-K. Bayesian updating of structural models and reliability using Markov chain Monte Carlo simulation. J Eng Mech 2002;128(4):380–91.
[30] Cheung SH, Beck JL. Bayesian model updating using hybrid Monte Carlo simulation with application to structural dynamic models with many uncertain parameters. J Eng Mech 2009;135(4):243–55.
[31] American Lifelines Alliance. Seismic fragility formulations for water systems part 1 - guideline. Washington D.C.: FEMA, ASCE; 2001, p. 104, https://www.americanlifelinesalliance.com/pdf/Part_1_Guideline.pdf.
[32] Federal Emergency Management Agency Mitigation Division. Hazus-MH technical manual: earthquake model. Washington D.C.: Department of Homeland Security; 2013, p. Chapter 8, https://www.fema.gov/media-library-data/20130726-1820-25045-6286/hzmh2_1_eq_tm.pdf.
[33] Blessing R, Sebastian A, Brody SD. Flood risk delineation in the United States: How much loss are we capturing? Natural Hazards Rev 2017;18(3):04017002.
[34] Atkinson GM, Boore DM. Recent trends in ground motion and spectral response relations for North America. Earthq Spectra 1995;6(1):15–35.
[35] Stan Development Team. Stan user's guide. 2016, https://mc-stan.org/docs/2_26/stan-users-guide/.

[36] Lemoine NP. Moving beyond noninformative priors: why and how to choose weakly informative priors in Bayesian analyses. Oikos 2019;128(7):912–28.
[37] Wang M, Takada T. Macrospatial correlation model of seismic ground motions. Earthq Spectra 2005;21(4):1137–56.
[38] Cohen S, Brakenridge GR, Kettner A, Bates B, Nelson J, McDonald R, Huang Y-F, Munasinghe D, Zhang J. Estimating floodwater depths from flood inundation maps and topography. J Am Water Resour Assoc 2018;54(4):847–58.
[39] Tate E, Muñoz C, Suchan J. Uncertainty and sensitivity analysis of the HAZUS-MH flood model. Natural Hazards Rev 2014;16(3):04014030.
[40] Reese S, Ramsay D. Riskscape: flood fragility methodology. Wellington, New Zealand: National Institute of Water and Atmospheric Research; 2010, p. 42.
[41] Floyd RW. Algorithm 97: shortest path. Commun ACM 1962;5(6):345.
[42] González AD, Dueñas-Osorio L, Sánchez-Silva M, Medaglia AL. The interdependent network design problem for optimal infrastructure system restoration. Comput-Aided Civ Infrastruct Eng 2016;31(5):334–50.
[43] Harmsen S, Frankel AD, Petersen M. Deaggregation of US seismic hazard sources: the 2002 update. USGS; 2003.
[44] National Oceanic and Atmospheric Administration. PDS-based precipitation frequency estimates with 90% confidence intervals (in inches). Department of Commerce, Washington D.C.; 2018, URL https://hdsc.nws.noaa.gov/hdsc/pfds/pfds_map_cont.html.
[45] Hoffman MD, Gelman A. The No-U-Turn sampler: adaptively setting path lengths in Hamiltonian Monte Carlo. J Mach Learn Res 2014;15(1):1593–623.
[46] Ortega Absil C, Riccardi A, Vasile M, Tardioli C. SMART-UQ: uncertainty quantification toolbox for generalised intrusive and non intrusive polynomial algebra. In: 6th international conference on astrodynamics tools and techniques, 2016.
[47] Baroud H, Barker K. A Bayesian kernel approach to modeling resilience-based network component importance. Reliab Eng Syst Saf 2018;170:10–9.
[48] Kullback S, Leibler RA. On information and sufficiency. Ann Math Stat 1951;22(1):79–86.
[49] Cavalieri F, Franchin P, Giovinazzi S. Earthquake-altered flooding hazard induced by damage to storm water systems. Sustaina Resilient Infrastruct 2016;1(1–2):14–31.
[50] Hart DE, Giovinazzi S, Byun D-S, Davis C, Ko SY, Gomez C, Hawke K, Todd D. Enhancing resilience by altering our approach to earthquake and flooding assessment: multi-hazards. In: 16th World Conference on Earthquake Engineering, 2018.
[51] Sela L, Amin S. Robust sensor placement for pipeline monitoring: Mixed integer and greedy optimization. Adv Eng Inform 2018;36:55–63.